Subproject B1.5

Decoherence-Free Materials for Superconducting Quantum Circuits: Fabrication and Characterization

Principle Investigators: Alexey Ustinov / Georg Weiss / Michael Siegel

CFN-Financed Scientists: **Alexey Feofanov (3/4 E13, 10.13 months, AG Ustinov),**
Stefano Poletto (1 E13, 2.5 months, AG Ustinov),
Adler Clemens (1/2 E13, 4 months, AG Weiss),
Torben Peichl (1/2 E13, 3 months, AG Weiss)
Stefan Wünsch (1 E13, 18 months, AG Siegel)

Further Scientists: **Ch. Kaiser (IMS), Dr. R. Schäfer (INT), Dr. J. Lisenfeld (PI)**

Physikalisches Institut (PI)
Karlsruher Institut für Technologie (KIT)

Institut für Mikro- und Nanoelektronische Systeme (IMS)
Karlsruher Institut für Technologie (KIT)

Decoherence-Free Materials for Superconducting Quantum Circuits: Fabrication and Characterization

Introduction and Summary

Superconducting quantum bits (qubits) are promising candidates for the implementation of quantum computers [1]. They offer various advantages over other types of qubits, such as scalability, integrability with classic electronics and free design of their characteristic parameters. Their main problem, however, lies in the fact that it has only been possible to fabricate superconducting qubits with limited coherence times so far. The latter should be long enough to carry out the necessary number of logic operations including quantum error-correcting codes for a real quantum calculation, which can be approximated to account for 10^4 [2].

The main decoherence mechanism in phase qubits, which consist of a superconducting ring interrupted by a Josephson junction (JJ) [3], was recently identified to come from two-level tunneling systems (TLS), which couple to the qubit and their quantum information [4,5]. The macroscopic manifestation of these TLS are dielectric losses [4,5]. Another type of decoherence comes from the control circuitry, for example the noisy current in the magnet coil determining the flux working point.

The goal of this subproject is twofold: On the one hand, we aim to improve the materials used for qubit fabrication and hence build phase qubits with improved coherence times. On the other hand, we aim at changing the qubit design in order to make the qubit less sensitive to certain types of decoherence or at developing new qubit architectures with increased operation speed, so that the required number of operations can be carried out in a shorter time.

At first, a fabrication technology for sub-µm to µm-size high-quality Nb/Al-AlO_x/Nb Josephson junctions was developed [B1.5:1]. A very high junction quality is crucial to exclude that any intrinsic loss mechanisms in the junctions contribute to decoherence. Samples fabricated with this new technology were successfully used for various quantum experiments [B1.5:2, B1.5:3], which showed that their quantum properties could be predicted from the design parameters with high precision. Phase qubits were also fabricated and characterized and exhibited coherence times which were longer than for most other phase qubits made of the same materials [B1.5:1].

These long coherence times are especially noteworthy as the qubit's insulation layer was made of SiO_x, which is a rather lossy dielectric. In order to identify insulating thin films with lower dielectric losses, which should help to further increase the coherence times, various materials which can be used in Josephson junction fabrication (partly provided by external collaborators) were investigated at 4.2 K. For this, a novel method for direct and quantitative loss measurements employing lumped element superconducting resonators was developed [B1.5:4]. This method also allows measuring the frequency dependence of the losses in the relaxation regime [B1.5:4]. Furthermore, several materials with lower losses than in SiO_x were identified, so that the fabrication of low-decoherence phase qubits should be possible in the future as soon as the corresponding deposition systems are installed in Karlsruhe.

The same measurement method was also used to probe the TLS properties in the qubit working regime at mK temperatures and single-photon powers. Since the behavior of the TLS in this regime is dominated by resonant absorption processes, we were able to probe the TLS density of states and found it to be frequency dependent [B1.5:5]. Although this dependence was predicted by theory [6]

and found in specific heat measurements [7], it had never been reported for dielectric loss measurements before. This result is important for qubit design, as it allows choosing the optimal qubit working frequency. While the measurement method discussed so far is suited to measure dielectric losses in bulk dielectrics, we were also interested in TLS surface states. For this, we carried out measurements in the qubit working regime using coplanar waveguide (CPW) resonators with different conductor materials and substrates. We found that the nature of the surface TLS is identical, independent of the employed materials [B1.5:6].

Furthermore, we have investigated new qubit architectures, which might help to increase the number of logical operations within the coherence time. For this, the newly developed fabrication technology for high quality Josephson junctions should also make designs possible which could not be successfully implemented so far due to an insufficient junction quality [B1.5:7].

Another approach was to shift the qubit working point. Flux qubits are usually biased to the working point by a weekly coupled external coil; this does not allow using superconducting shields, which are an excellent tool to protect a qubit from high-frequency noise. π-shifters based on junctions with a ferromagnetic interlayer (SFS) can be a useful tool for individual qubit bias especially in multi-qubit circuits. π-shifters also relax the requirement that the size of every qubit loop must be controlled precisely. We found that the usage of such ferromagnetic layers does not reduce the qubit coherence times [B1.5:8].

In order to increase the operation speed and hence increase the ratio of operations per coherence time, we have also developed a new manipulation scheme. This employs a double SQUID as the qubit and does not require the use of microwaves. We have demonstrated operation speeds up to 26 GHz [B1.5:9]. Furthermore, we could show that the coherence times obtained by this new operation technique were identical to those obtained by classic microwave manipulation [B1.5:10], so that it can be said that no additional decoherence is introduced due to our novel method.

1. Fabrication Technology for phase qubits with long coherence times

A high quality of the Josephson junctions is crucial for the fabrication of superconducting qubits with long coherence times. Especially, high subgap leakage can lead to decoherence [8,9]. Furthermore, a small junction size can be useful for low-decoherence qubits as the major part of the losses can be transferred to shunt capacitors. Finally, the Nb/AlO_x/Nb fabrication technology offers various advantages over Al based devices, such as better scalability, better integrability, more design freedom and a generally more mature technology. Consequently, we have developed a fabrication process for sub-µm to µm-size Nb/Al-AlO_x/Nb Josephson junctions of high quality [B1.5:1]. This involved minimizing the Nb film stress, determining new etching parameters and, as the main point, the development of an Al hard mask technique for the JJ definition. Usage of this novel method avoids further chemical processes, which might create additional TLS systems on the film surfaces.

High quality JJs with sizes down to 0.5 µm² could be fabricated with a precisely defined JJ area. Figure 1 shows the *IV* curve of a typical junction, here with a critical current density of j_c = 660 A/cm². The quality parameters (obtained at T = 4.2 K) for all junctions typically accounted for $I_cR_N \approx 1.8$ mV, $R_{sg}/R_N > 30$ and $V_{gap} > 2.8$ mV, which indicates an exceptionally high quality. Here, I_c is the critical current, R_{sg} the subgap resistance at 2 mV, R_N the normal resistance and V_{gap} the gap voltage of the JJ. Detailed measurements of the subgap regime showed that the decoherence mechanism due to quasiparticle leakage in quantum devices containing our JJs should be negligible.

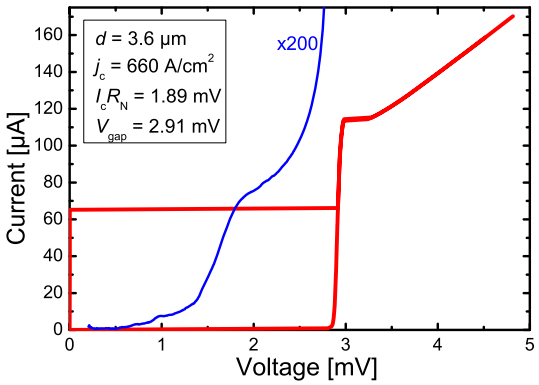

Figure 1: *IV* curve of a typical Josephson junction fabricated with the newly developed Nb/Al-AlO_x/Nb technology, measured at T = 18 mK. The subgap branch was measured with an applied magnetic field, a voltage bias setup and is magnified by a factor of 200.

As a first test for the usability of our junctions for quantum experiments, the size dependence of macroscopic quantum tunneling (MQT) was investigated experimentally [B1.5:2]. We found a clear and systematic variation of the crossover temperature T_{cr} with JJ area, which had never been reported before. The resulting experimental values between T_{cr} = 147 mK and T_{cr} = 362 mK could be predicted by the sample design parameters with high precision, which shows that the quantum properties of our JJs can indeed be designed at will.

Since phase qubits often contain shunting elements like capacitors C or inductors L to tune the qubit working point or decouple the qubit from its impedance environment, respectively, we also investigated the quantum dynamics of LC shunted JJs [B1.5:3]. A recently developed theory [10] predicts that such a complex system should be described by a two-dimensional potential and hence exhibit two energy scales (equivalent to two plasma frequencies ω_p). By microwave spectroscopy experiments, we observed both plasma modes in one sample, which was the first experimental proof of this effect. These results have to be considered in qubit design and operation in the future. Furthermore, we found that the lower plasma mode can be designed as a very flat function of the bias current I through the junction. This should help to create phase qubits which are less sensitive to dephasing, since the dephasing rate is given by $\Gamma_\phi \approx \Delta I_n (\partial\omega/\partial I)$, where ΔI_n is the amplitude of the low frequency current noise.

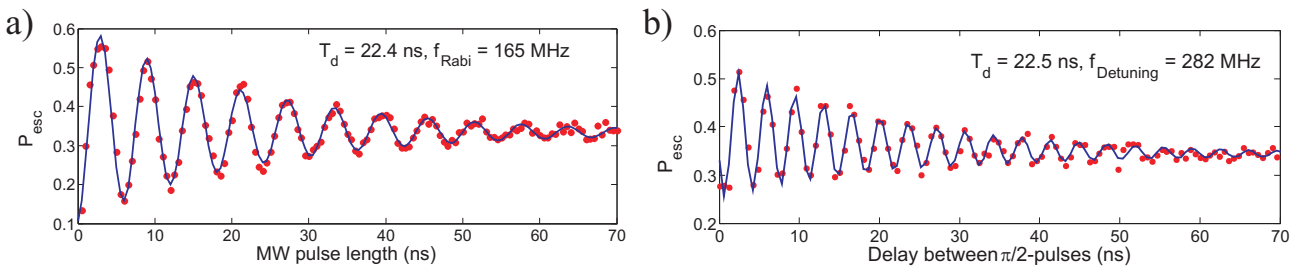

Figure 2: Characteristic measurements on one of our phase qubits. a) Rabi oscillations with a decay time of 22.4 ns. b) Ramsey fringes with an applied microwave detuned by 282 MHz from the qubit level splitting. Here, a dephasing time of 22.5 ns was found.

The newly developed technological process was also used to fabricate phase qubits. They were characterized in a dilution fridge setup, which had been used commercial suppliers before for measurements on Nb/Al-AlO_x/Nb phase qubits fabricated by three different. The commercial samples exhibited coherence times below 8 ns. On our qubits, typical experiments like the observation of Rabi oscillations (coherent oscillations between the qubit states $|0\rangle$ and $|1\rangle$),

relaxation from $|1\rangle$ to $|0\rangle$ and Ramsey-type experiments (rotation by a $\pi/2$ pulse to the equatorial plane of the Bloch sphere, waiting a certain time and rotation by another $\pi/2$ pulse) were carried out. The Rabi oscillations in one of our samples (having a qubit level splitting of around 13 GHz) are shown in Figure 2a. It can be seen that the observed coherence time of 22 ns exceeds the ones obtained with commercial samples by far. In more detail, a relaxation time of $T_1 = 26$ ns was found and various Ramsey-type experiments led to an average dephasing time of $T_2 = 21$ ns. These values are also longer than those obtained on other Nb/Al-AlO_x/Nb phase qubits of similar design reported in literature. Characterization of a second qubit having a level splitting around 23 GHz proved to be more difficult, since this frequency was above the upper specification frequency of the employed RF cables. Even though, the obtained relaxation time of $T_1 = 11$ ns is still longer than for all commercial samples at much lower frequencies. The reason why the coherence time of the higher frequency qubit is shorter will be discussed in more detail in chapter 3.

Altogether, we attribute our long coherence times to the excellent Josephson junction quality. Since we used the rather lossy dielectric SiO_x in our fabrication process (see next chapter), it can be expected that the coherence times can be significantly improved by the implementation of low-loss fabrication processes in Karlsruhe, such as would be possible with an inductively coupled plasma (ICP) system, which was a suggested investment in the project proposal.

2. Possible low-loss dielectric materials for qubit fabrication

As discussed in the previous chapter, we have excluded the possibility that the decoherence in our phase qubits might be caused by intrinsic leakage currents in the JJ. Instead, the major loss mechanism should be due to coupling of the qubit to spurious two-level systems (TLS) in the qubit's vicinity, as suggested by Martinis *et al.* [4,5]. Since the macroscopic manifestation of these TLS are dielectric losses tan δ, measurements of the latter are an appropriate tool to identify low-decoherence materials for qubit fabrication. The natural tool of choice for this are superconducting resonators, as they allow characterizing the dielectric materials using the same fabrication technology, temperatures and frequencies as used for the qubits.

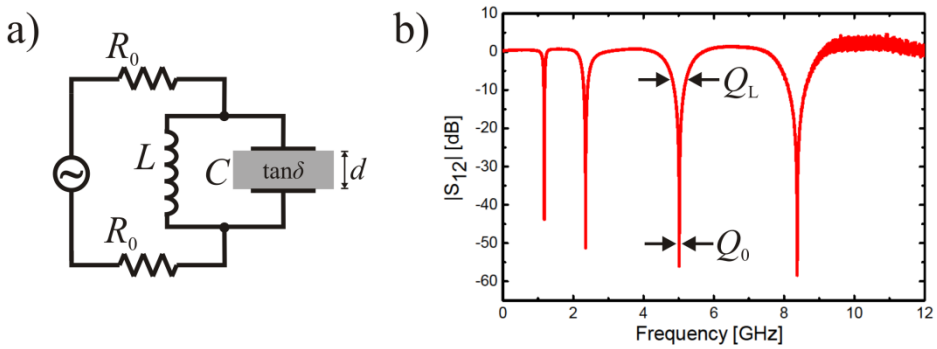

Figure 3: a) Schematics of the LC circuit used for measurements of dielectric losses. b) Exemplary measurement with four multiplexed resonators, here with SiO as dielectric, with illustration of the loaded quality factor Q_L and the intrinsic quality factor Q_0.

We have developed a method for reliable, direct, quantitative and frequency-dependent measurements of dielectric losses in amorphous thin films using lumped element (LE) resonators [B1.5:4]. Its simple schematic architecture can be seen in Figure 3a. It results in a notch-like resonance dip, so that the intrinsic quality factor Q_0 can be directly extracted from the measurement data (see Figure 3b). Due to the fact that superconductors are used as the conductor material, the only remaining losses are caused by the dielectric so that we find tan $\delta = 1/Q_0$. This resonator

architecture also allows multiplexing of the resonators by putting them in series, so that various frequency points can be measured in one cool-down (see Figure 3b), which is especially important for time-consuming dilution fridge measurements (see next chapter).

This newly developed method was used to measure the frequency dependent dielectric losses in various thin films which can be used in JJ fabrication at $T = 4.2$ K. At this temperature, the losses are dominated by relaxation processes. Although it is not the regime in which qubit measurements are carried out, the comparison between different materials will not change with temperature and can be directly applied to qubit fabrication processes. It can be seen in Figure 4 that at a constant temperature of 4.2 K all materials show a weak frequency dependence which is consistent with predictions of the tunneling model for the temperature range below the so-called 'plateau-region'. On the other hand, this behavior is also in agreement with a power law [11] $\tan\delta \propto \omega^{n-1}$ with exponents of $n \approx 0.6$. This value is claimed to be characteristic for relaxation of dipoles exhibiting many-body interactions [12] and to be applicable to glass-like materials. So far, the TLS responsible for qubit decoherence have not been assumed to be interacting, so that this latter interpretation might be considered in such theoretical models.

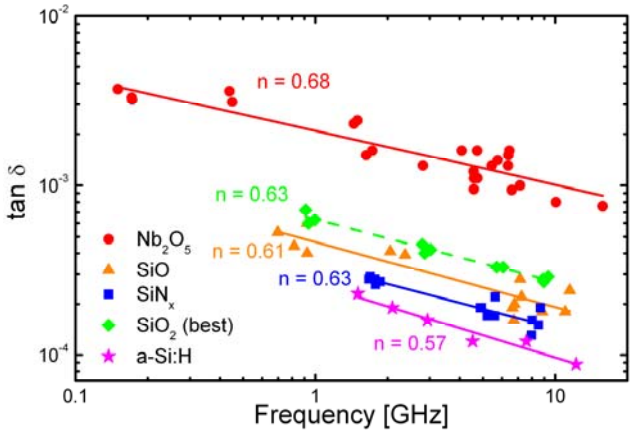

Figure 4: Frequency dependent dielectric losses in various amorphous thin films which can be used in Josephson junction fabrication. Data were measured at 4.2 K.

Furthermore, our results allow comparing the losses in different materials to each other. We found that the materials used in the JJ fabrication process at the IMS, namely Nb_2O_5 (created by anodic oxidation) and thermally evaporated SiO_x, are rather lossy. Additionally, even a thorough optimization of the deposition parameters did not result in RF sputtered SiO_2 with lower losses than in SiO, so that the latter remained the material employed for JJ fabrication. Some of the investigated dielectrics were provided by external collaborators, such as SiN_x (by the PTB Braunschweig) and a-Si:H (by the CNR Naples, Italy). It can be seen in Figure 4 that these materials exhibit much lower losses than the materials used for qubit fabrication at the IMS. However, phase qubits fabricated at the PTB using SiN_x as dielectric also only showed coherence times around 7-8 ns. This supports our conclusion that the losses in the PTB phase qubits are rather due to an insufficient JJ quality, while the long coherence times around 25 ns in our qubits are due to the excellent JJ quality and only limited by the lossy SiO_x. This means that the usage of low-loss dielectrics in our fabrication process should indeed result in significantly increased coherence times.

3. Probing the TLS properties using superconducting resonators

The same measurement method, as described in the previous chapter, was also used to probe the TLS properties in the qubit working regime at mK temperatures and at powers where single photon

processes should dominate. Here, the dielectric losses are dominated by resonant absorption processes, i.e. only the TLS of energy equal to the resonance frequency contribute to the losses. Since the occupation of the lower and upper energy level of these TLS scales with the external energy supplied to the system, the losses depend on temperature T and applied MW power P like [6]

$$\tan\delta = 4\pi\alpha\omega\left(1+\frac{P}{P_c}\right)^{-\frac{1}{2}}\tanh\left(\frac{\hbar\omega}{2k_BT}\right), \qquad (1)$$

where P_c is the saturation power, ħ Planck's reduced constant and k_B the Boltzmann constant. The value of α is given by

$$\alpha = \frac{\pi n p^2}{3\varepsilon_r}, \qquad (2)$$

where p is the dipole moment of the TLS, ε_r the dielectric permittivity and $n(E)$ the TLS density of states (DOS). The latter was predicted to be weakly energy dependent [6] in agreement with specific heat measurements [7] but this was never explicitlty confirmed in investigations of dielectric losses.

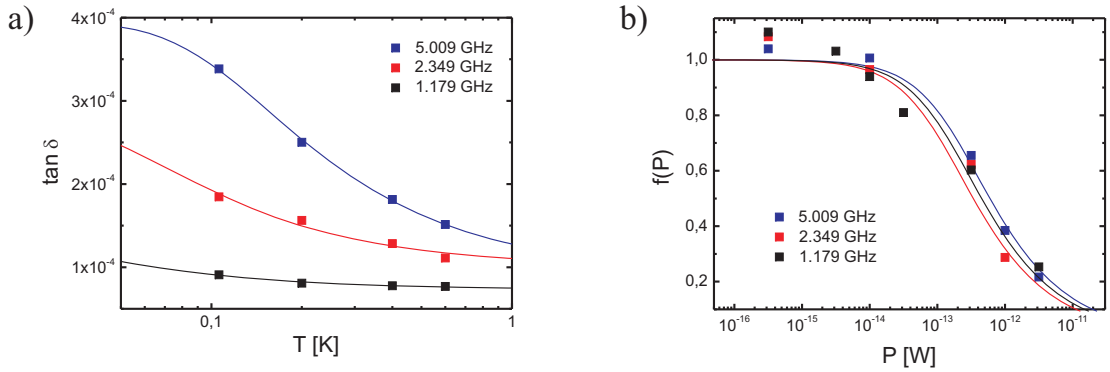

Figure 5: a) The temperature dependence of the dielectric losses in SiO_x is in good agreement with equation (1) in the low power limit for all investigated frequencies. b) The same is true for the power dependence. The tentatively determined exponents of the power term in (1) were in the range of -0.9 to -0.4, which is in good agreement with the theoretical value of -0.5 in Eq.(1).

As we wanted to probe the energy dependence of the TLS DOS, we carried out LE resonator measurements (as described in the previous chapter) on SiO_x in the resonant absorption regime (i.e. in a dilution refrigerator at low MW powers). For this, our newly developed method proved to be very advantageous, since it allowed measuring several resonators in one cooldown cycle (see Figure 3). This was made possible by the development of a broadband measurement setup [B1.5:5] including a home-made broadband amplifier and a home-made power combiner.

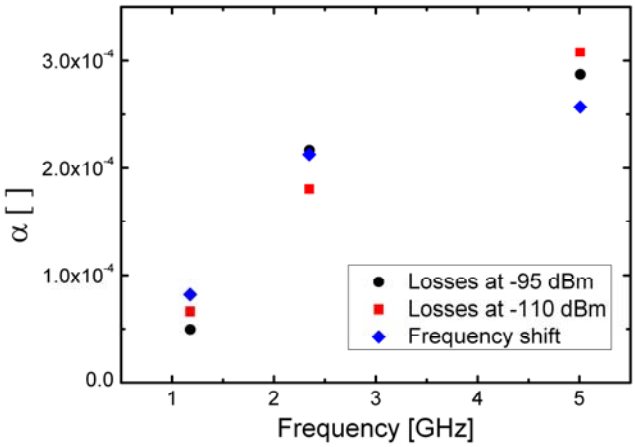

Figure 6: The prefactor α in equation (1) versus resonance frequency of the superconducting LE resonators. This is a direct measure for the energy dependence of the TLS DOS.

As a first result, we could reproduce equation (1) in our measurement results with a very good agreement (see Figure 5), which shows that the loss behaviour is indeed well described by the resonant absorption model. Furthermore, the corresponding fits were used to determine the prefactor α. Since the only frequency dependent parameter in equation (2) is the TLS density of states n, plotting α over frequency will allow probing the energy dependence of the latter. This is shown in Figure 6, where it is visible that the DOS monotonically increases with energy. In fact, the energy dependence extracted from our data that way is much stronger than predicted theoretically for glasses [6,7]. On the other hand, the numbers obtained from loss measurements agree well with resonance frequency shift measurements (for details see [B1.5:5]). This might be the first time that this energy dependence of the TLS DOS was found in loss measurements experimentally – which is even more important as the experiments were done with materials, frequencies and experimental conditions similar to those used for superconducting qubits. Additionally, these findings are in excellent agreement with the observation of shorter coherence times at higher qubit frequencies reported in chapter 1. Altogether, these results are important for qubit design, since it seems advantageous to build qubits operating at frequencies with a low density of TLS.

We have also investigated the TLS properties at 2.5 GHz with the use of $\lambda/2$ CPW resonators on crystalline substrates [B1.5:6], where no amorphous dielectrics are present. Consequently, the object of study are the TLS on metal surfaces, which might also play an important role in qubit decoherence. Here, the analysis of the measurement data is more subtle, since first, only a fraction of the electric field is stored in the TLS hosting material, and second, only the loaded quality factor Q_L could be measured. Consequently, the loss rate δ was determined, which is not equivalent to the tan δ values of the TLS under investigation.

However, as can be seen in Figure 7, the temperature and power dependence of the loss rate does also obey the resonant absorption formula (1). Apparently, the expected relaxation absorption does not add any further temperature dependence in this regime. The fits with (1) showed that the values of the prefactor α were of the same order of magnitude for all used substrates (sapphire and silicon) and superconductors (Al and Nb), indicating that the DOS of TLS surface states is universal. This material independence leads to the suggestion that the nature of these TLS lies in general surface/interface states.

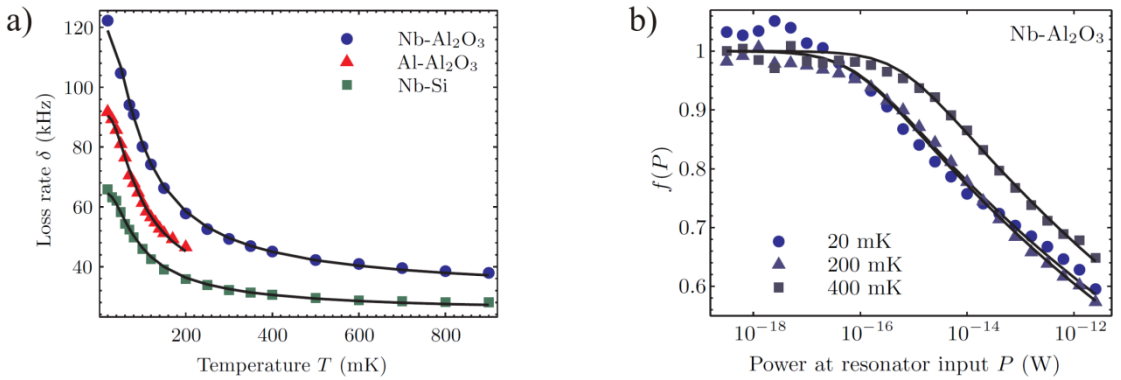

Figure 7: a) The temperature dependence of the loss rate at 2.5 GHz in CPW resonators is in very good agreement with equation (1). b) Also the power dependence is well described by the corresponding term in equation (1).

4. Implementation of π-shifters based on superconductor-ferromagnet-superconductor Josephson junctions

The fundamental property of superconducting weak links is a 2π-periodic current-phase relation. The supercurrent through a conventional Josephson junction is usually described by the harmonic relation $I_s = I_c \sin \varphi$, where I_c is the critical current. The so-called Josephson π-junction [13, 14] has the inverse current-phase relation $I_s = I_c \sin(\varphi+\pi) = -I_c \sin \varphi$. Embedding a π-junction into a superconducting loop leads to self-biasing of the loop by a spontaneously induced supercurrent. Providing the π-junction's critical current I_c is chosen to be much larger than that of conventional 0−junctions employed in the very same loop, the phase difference across the π-junction is always close to π even at zero magnetic field.

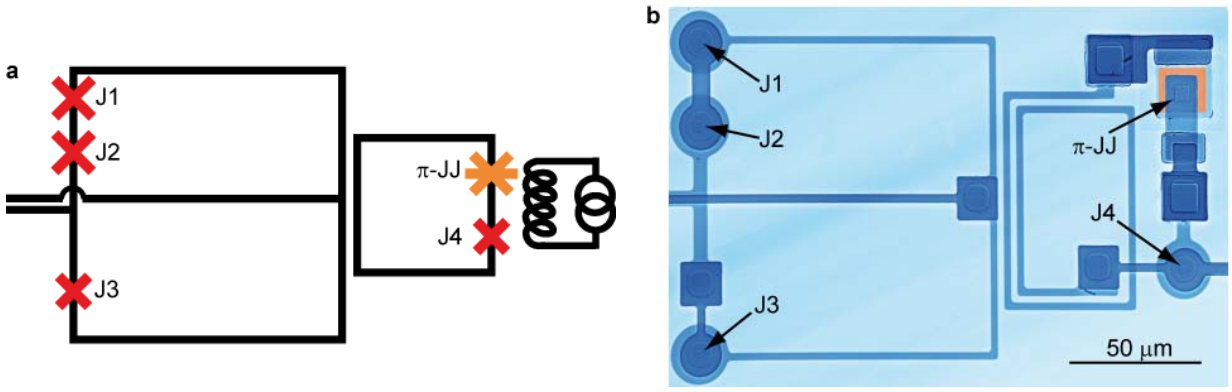

Figure 8: Self-biased phase qubit. **a**, Schematic of a phase qubit circuit used to test the decoherence properties of the π-junction. The qubit is realized by the central loop with embedded conventional and π-Josephson junctions. The larger loop to its left is a dc-SQUID for qubit readout. To the right of the qubit is a weakly coupled flux bias coil. **b**, Scanning electron microscope picture of the realized phase qubit employing a π-junction in the qubit loop. The flux bias coil is not shown.

The usage of π-junctions as passive phase shifters [B1.5:8] offers an advantage for the operation of superconducting flux qubits at the degeneracy point requiring zero or a very small external magnetic field. Potentially, this allows noise and electromagnetic interference induced by magnetic field sources to be minimized. The answer to the question of whether or not π-junctions can become useful in superconducting circuits designed for quantum computing applications depends on their impact on the coherence properties of the qubits. Potential sources of decoherence introduced by π-

junctions can for instance be spin-flips in the ferromagnetic barrier, either occurring randomly or being driven by high-frequency currents and fields, as well as the dynamic response of the magnetic domain structure. We address these important coherence issues in an experiment, in which we use a π-junction realized using superconductor-ferromagnet-superconductor (SFS) sandwich technology [15] to self-bias a superconducting phase qubit. We have chosen here a phase qubit rather than a flux qubit [16] due to the simpler fabrication procedure for the former. The results reported below would nevertheless remain fully applicable to flux qubits.

A phase qubit consists of a single Josephson junction embedded in a superconducting loop. It is magnetically biased close to an integer number of flux quanta in the loop. At such a bias, the potential energy of the qubit exhibits an asymmetric double-well potential, whereas two quantized energy eigenvalues of the phase localized inside the shallow well only are used as the logical qubit states $|0\rangle$ and $|1\rangle$. Figure 8a shows a circuit schematic and 8b a micrograph of the tested sample. Here, a π-junction is connected in series to the phase qubit's tunnel junction. Coherent qubit operation is demonstrated by the data reported in Figure 9a, showing Rabi oscillation of the excited qubit state population probability versus the duration of a resonant microwave pulse. The oscillations exhibit a decay time of about 4 ns, which is a typical value reachable in samples fabricated using similar fabrication processes. To find out whether the π-junction does introduce additional decoherence, a conventional phase qubit without a π-junction was fabricated on the same wafer. As shown in Figure 9b, this reference qubit shows a nearly identical decay time for Rabi oscillations, allowing us to conclude that at least on the observable time scale no extra decoherence is introduced by the SFS π phase shifter employed in this circuit and that the decoherence in both qubits is limited by some other mechanism.

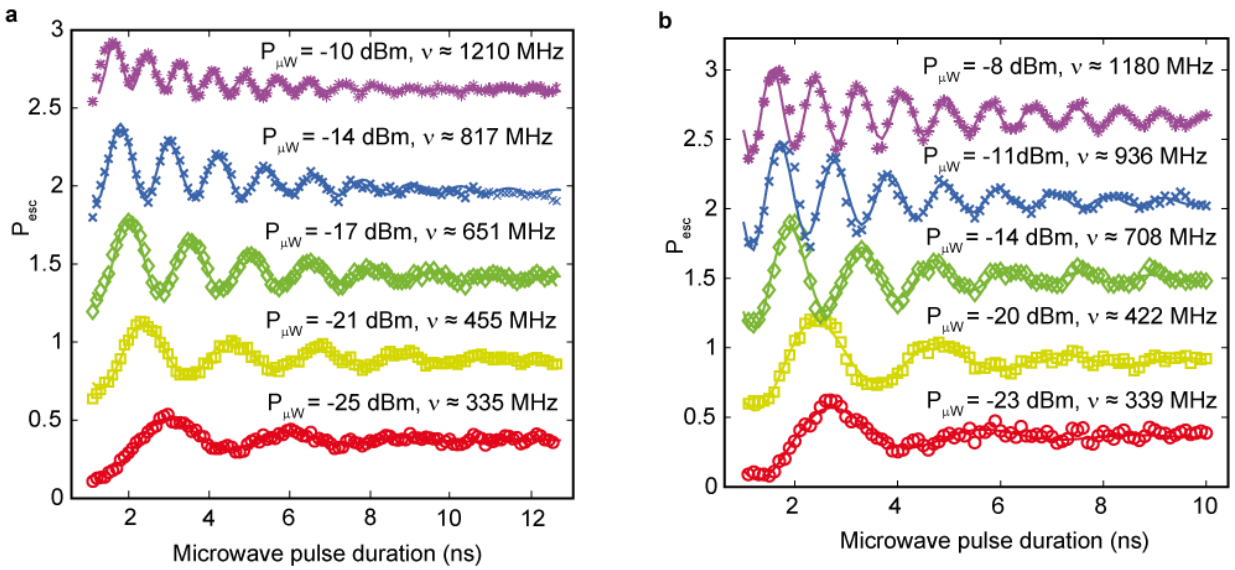

Figure 9: Rabi oscillations between the ground and the excited qubit states resulted from resonant microwave driving. **a**, Observed in the phase qubit with embedded π-junction, and **b**, A conventional phase qubit made on the same wafer as a reference. Each data set was taken using the indicated microwave power as delivered by the generator, giving rise to a change in the coherent oscillation frequency as expected for Rabi oscillations.

5. Experimental investigation of a "microwave-free" manipulation technique to increase the speed of operation in a superconducting qubits

In parallel to the research on materials aimed at increasing the coherence time of solid states quantum bits fabricated by our groups, we are working on new techniques of manipulation to increase the speed of operation of our devices. Longer coherence times in combination with a faster manipulation allow reaching the final goal of 10^4 operations within the coherence time in a shorter total time.
The device under study is a double-SQUID, namely a superconducting loop interrupted by a dc-SQUID, which can be approximated as a Josephson junction with a tunable critical current. A schematic representation of the device is shown in Figure 10a. The system can be manipulated via two fluxes Φ_c and Φ_x that control, respectively, the height of the barrier between the two minima (Figure 10b) and the symmetry of the potential (Figure 10c). The investigated sample was fabricated by an external foundry.

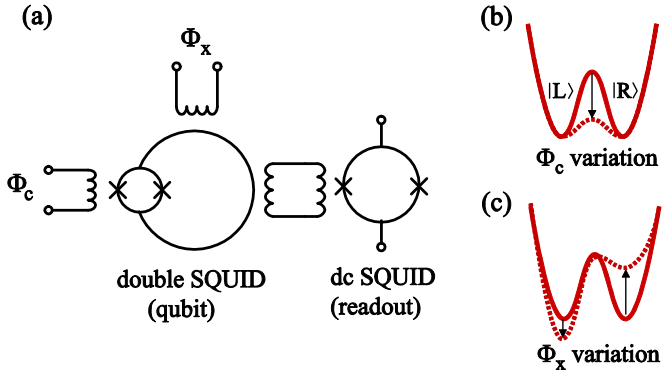

Figure 10: Schematic representation of the device under study (a). The double-SQUID can be manipulated via the two fluxes Φ_c and Φ_x. The bias flux Φ_c changes the height of the barrier between the two minima (b), while the flux Φ_x changes the symmetry of the system (c).

We demonstrated that the device can be manipulated without using microwaves measuring tunable coherent oscillations at frequencies ranging from 6 to 26 GHz [B1.5:9], with a theoretical upper limitation defined by the layout of the double-SQUID. The manipulation of the qubit is performed via a continuous modification of the energy potential profile via the two control fluxes Φ_c and Φ_x, exploiting both double and single well potential configurations. The manipulation of the energy profile can be seen in Figure 11a, together with the sequence of bias values and readout dc-SQUID currents used to realize it. The energy potential of the qubit is deformed into a single well by a fast pulse Φ_c^{pulse} for a variable time Δt.

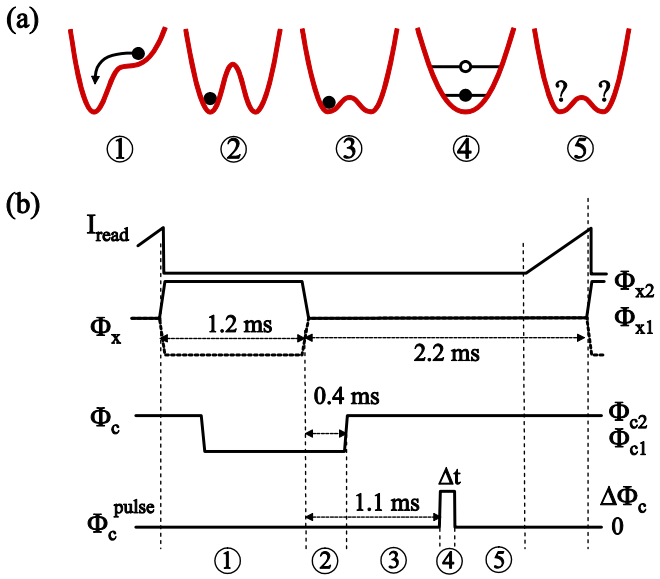

Figure 11: (a) Variation of the potential shape during the manipulation. (b) Sequence of the readout dc-SQUID current and flux bias values. The solid and dashed lines in the Φ_x curve correspond to initialization in the opposite potential wells.

The measured oscillations between the two minima in a double well situation versus the time Δt of the fast pulse Φ_c^{pulse} are reported in Figure 12. Theoretically, these oscillations correspond to Larmor oscillations between the lowest two energy levels of the system in the single well potential, projected in the base of left $|L\rangle$ and right $|R\rangle$ (the base of the persistent circulating current). In addition, the frequency of oscillation can be tuned by changing the amplitude of the fast pulse Φ_c^{pulse} (Figure 12).

This manipulation technique leads to the major advantage of a relaxed requirement for the coherence time to implement error correction algorithms. Moreover, the system has low sensitivity to both control fluxes Φ_x and Φ_c, so that the qubit is protected against flux noise.

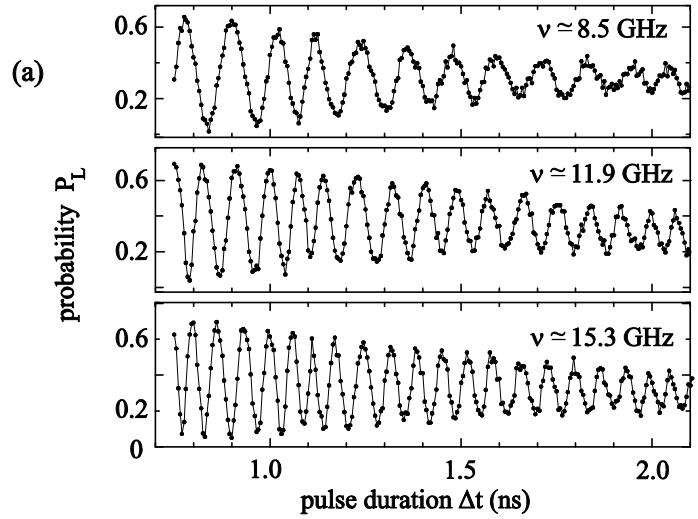

Figure 12: Dependence of the probability of measuring the state $|L\rangle$ on the pulse duration Δt for different pulse amplitudes

To prove that our new manipulation scheme does not influence the coherence time of the system, we manipulated the device as a phase qubit by controlling the quantum evolution via resonant microwave pulses [B1.5:10]. The coherence time of the measured Rabi oscillations and the

relaxation time T_1 are compatible with the coherence time measured in the manipulation without microwaves, proving that the main sources of decoherence must be searched in the fabrication materials and not in this particular manipulation technique.

References

- own work with complete titles -

[1] Yu. Makhlin, G. Schön, and A. Shnirman, Rev. Mod. Phys. **73**, 357 (2001)

[2] E. Knill, R. Laflamme, and W. H. Zurek, Science **279**, 342 (1998)

[3] R. W. Simmonds, K. M. Lang, D. A. Hite, S. Nam, D. P. Pappas, and J. M. Martinis, Phys. Rev. Lett. **93**, 077003 (2004)

[4] J. M. Martinis, K. B. Cooper, R. McDermott, M. Steffen, M. Ansmann, K. D. Osborn, K. Cicak, S. Oh, D. P. Pappas, R. W. Simmonds and C. C. Yu, Phys. Rev. Lett. **95**, 210503 (2005).

[5] R. McDermott, IEEE Trans. Appl. Supercond. **19**, 2 (2009).

[6] W. A. Phillips, Rep. Prog. Phys. **50**, 1657 (1987)

[7] R. B. Stephens, Phys. Rev. B **8**, 2896 (1973)

[8] M. A. Gubrud, M. Ejrnaes, A. J. Berkley, R. C. Ramos Jr, I. Jin, J. R. Anderson, A. J. Dragt, C. J. Lobb and F. C. Wellstood, IEEE Trans. Appl. Supercond. **11,** 1002 (2001)

[9] F. P. Milliken, R. H. Koch, J. R. Kirtley and J. R. Rozen, Appl. Phys. Lett. **85**, 5941 (2004)

[10] G. Rotoli, T. Bauch, T. Lindström, D. Stornaiuolo, F. Tafuri, and F. Lombardi, Phys. Rev. B **75**, 144501 (2007).

[11] A. K. Jonscher, J. Phys. D: Appl. Phys. **32**, R57 (1999)

[12] K. L. Ngai, A. K. Jonscher and C. T. White, Nature **277**, 185 (1979)

[13] L. N. Bulaevskii, V. V. Kuzii, and A. A. Sobyanin, JETP Lett. **25,** 290 (1977)

[14] A. I. Buzdin, L. N. Bulaevskij, and S. V. Panyukov, JETP Lett. **35,** 178-180 (1982)

[15] V. V. Ryazanov *et al*., Phys. Rev. Lett. **86,** 2427 (2001)

[16] I. Chiorescu, Y. Nakamura, C. J .P. M. Harmans, and J. E. Mooij, Science **299,** 1869 (2003)